Deutscher Luft- und Raumfahrtkongress 2010
DocumentID: 161222

Mission Performance Optimization via Morphing Wing-Tip Devices

J. Wittmann and M. Hornung
Bauhaus Luftfahrt e.V., Lyonel-Feininger-Str. 28, 80807 München, Germany

H. Baier
Institute of Lightweight Structures, Technische Universität München,
Boltzmannstr. 15, 85748 Garching, Germany

Summary

Variable geometry wing-tip devices are considered to be a technology with high potential to improve aircraft performance. However induced drag reduction benefits suffer from penalties on aircraft level like increased wetted area, additional weight or power consumption. For the development of morphing technologies, the capability of a net-benefit assessment on aircraft level considering multiple flight performance optimization objectives within a single aircraft mission is essential. The purpose of this paper is to present aircraft flight performance improvements due to morphing wing-tips for a broad range of applications. For this study, the impacts of geometry adaption of a morphing wing-tip is considered and compared to a conventional rigid wing-tip rather than alternative wing-tip devices. Parameter studies and mission performance simulations are performed for the assessment of the morphing wing-tip degrees of freedom twist, camber and cant angle. Furthermore, the application of a methodology for morphing net-benefit assessment on aircraft level, including various performance metrics is presented.

1 Introduction

Increasing the aircraft efficiency and simultaneously reducing the environmental impacts are persistent design requirements for future civil aircraft. On the other hand, a growing tendency of aircraft operators towards life-time extensions of successful aircraft families, like the Airbus A320 or the Boeing B737, are noticeable. Subsequent modifications of the initial basic designs, like increasing MTOW and range, to fit current market requirements lead to a sub-optimal flight performance compared to an optimized design. Furthermore, rigid aircraft off-design operations, for example due to flight guidance or new environmental restrictions also result in performance drawbacks.

Future military aircraft demands tend towards multi-role mission unmanned areal vehicles (UAV) and by this to increase significantly the range of capabilities of the aircraft systems. Adapting and changing the wing shape in flight (morphing) would enable an air vehicle to perform multiple tasks in a single mission, increase mission performance and maneuverability, and radically expanding its flight envelope.

A potential technology to retrofit existing civil aircraft platforms as well as to open up advanced functionalities for military aircraft are adaptive wing-tip devices or winglets. The concept of rigid vertical endplates or winglets to reduce drag is not a new idea. Decades ago, *Cone* [1] and *Jones* [2] introduced the theory of non-planar lifting systems to alter the global flow pattern and thus to reduce induced drag. *Whitcomb* [3] first introduced a design concept of a near-vertical winglet that features an airfoil to alter the global flow field. This wing-tip concept reap the induced drag benefit, while simultaneously keeps the profile drag low. The result is a net-benefit which can generate a significant performance gain of

- 3-5% fuel burn reduction [4],
- buffet boundary improvement,
- Drag divergence Mach number increase,
- noise reduction and increased safety margins during high-lift operation (e.g. take-off and landing),

especially when off-design aircraft wings are considered. However, the subsequent integration of a winglet at conventional wings led also to significant aeroelastic problems like flutter which have to taken into account.

Adaptive wing-tip devices promise a further expansion of these potential benefits by adapting their geometry or significantly morph their shape. Several concepts have been developed to maintain optimum drag reduction capability even at changing flight conditions or to realize additional functionalities like load control or primary flight control. To realize this, numerous concepts to change the shape of winglets in flight have been patented by aircraft manufacturers like Airbus and Boeing [5–8].

The University of Bristol investigates adaptive wing-tip devices ("Morphlets") for broad flight control applications. *Ursache et al.* [9] analyzed a morphing wing-tip device intended for induced drag reduction that features several degrees of freedom (DoF) like tip dihedral, twist, taper and span. It has been demonstrated, that the specific air range of an aircraft designed for a 1,000nm mission can be increased in the order of 3.3-8.8%.

The application of morphing wing-tips for primary flight control as an alternative to the conventional flight control is demonstrated in [10] and [11]. The concept consists of a pair of winglets that are independently adjustable in cant angle to generate multi-axis coupled control moments [11]. Further improvement of the concept by using articulated split wing-tips (four independent multi-axis effectors) instead of a pair of single

winglets leads to increased redundancy in the primary flight control system. This could be exploited to realize additional functionalities such as drag or bending moment reductions [10].

NASA is working on biologically inspired non-planar wing designs referred to as Hyper-Elliptic Cambered Span (HECS) wing due to its continuous span-wise curvature [12]. It has been demonstrated by wind-tunnel tests that this wing design achieves a 15% increase of the lift-to-drag ratio compared to an optimum conventional planar wing having the same aspect ratio and wing span [12, 13]. Additionally, the HESCS wing features a continuous moveable outer wing-tip (30% semi-span) with a morphable trailing edge for pitch-, roll and yaw control.

Another application of morphing wing-tips was presented within the national funded German research project "Smart Winglets" in 2001. The morphing winglet developed in this project, offers active twist or camber for wing load reduction, performance driven airflow control and low noise drag generation (air brake) without lift decrease [14]. Different structural approaches (discrete conventional trailing edge tab, active smart structure, and a passive aeroelastic tailoring) have been investigated in more detail.

2 Motivation and Approach

Adaptive and morphing wing-tip concepts have been developed and applied for a broad range of applications. Commonly applied structural approaches for morphing technologies like

- rigid body mechanisms,
- smart material embedded composite structures,
- active aeroelastic structures,
- or compliant structures

can suffer from integration penalties on aircraft level like additional weight and drag or small impacts on the overall performance. For technology assessment, and to demonstrate the full potential of morphing systems, an overall approach for aircraft level benefit assessment is required. The advantage of this approach is the inclusion of the following aspects in the morphing technology assessment:

- Operational performance assessment of morphing technology driven wing-tip DoF on aircraft level.
- Flight and mission aircraft performance analysis.
- Impact analysis of a single morphing DoF contributing to an all-morphing wing-tip concept.
- Overall net-benefit assessment of a multi-objective application of a morphing wing-tip.

This paper presents a comprehensive approach consisting in the combination of the most important morphing wing-tip DoF in a single model combined with a single-mission-segment optimization this allows for evaluation of the overall performance benefits of the morphing system. The performance of an all-morphing design provides the upper boundary and acts as an absolute reference for a variety of quantitative assessments. It serves as a benchmark for any single morphing wing-tip parameter or morphing technology and enables the establishment of a benchmark representing the overall optimum for any mission composed of mission segments. As a result, the quantitative assessment of various morphing strategies will provide a "technology pull" for the most promising realization of morphing parameters. Alternatively, the quantitative assessment of morphing technologies will support a "technology push" for the most impacting realization in a particular application.

The focus of this paper is to demonstrate the performance improvements of changing conventional rigid wing-tips to adaptable ones. The first part of this paper describes a modeling approach for adaptive or morphing structures within aircraft conceptual design. Flight performance studies show the effects of an integrated morphing wing-tip into an aircraft model. Therefore, several flight performance optimization objectives are considered to adapt the geometry of the morphing wing-tip accordingly. In the second part of this paper, a multi-objective mission simulation shows the aerodynamic benefits of a morphing wing-tip during in-flight operation. A methodology introduced in [15] is applied to the optimization problem for overall mission performance calculation. Finally, a summary of the most impacting morphing wing-tip parameter is presented.

3 Morphing Aircraft Modeling

For the simulation of the morphing wing-tip performance on aircraft level an aircraft model including a morphing wing-tip is developed. The model accounts for major aircraft conceptual design disciplines like aerodynamics and structures and is composed of basic aircraft systems like wing, fuselage, horizontal tail and engines. The modeling fidelity is based primarily on aircraft conceptual design semi-empirical methods [16–18]. This represents an adequate compromise between accuracy and computational effort.

The aircraft model has been subsequently adapted to a morphing aircraft simulation model by implementing a geometry optimization loop and a flight mechanics module.

3.1 Reference Configuration

As the reference configuration for modeling, the Embraer 145-LR regional jet has been selected due to its broad operating range and its versatile use for civil and military applications. The aircraft is powered by two Rolls-Royce AE3007A1 engines with an installed flat rated static thrust of 33kN (ISA $+30^\circ$) at sea level. Basic reference aircraft parameters are given in TAB. 1.

TAB 1: Reference configuration basic parameters [19, 20]

Parameter	Value
MTOW	22t
OWE	12.11t
Maximum cruise speed	Ma 0.78
Reference wing area	51.18m^2
Span	20.04m
Leading edge sweep	26.5°
Relative wing thickness	11%
Taper ratio	0.231
Aspect ratio	7.82

For all performance studies presented below, an aircraft configuration take-off weight of 20t, including a payload of 4t and a fuel load of 3,886kg have been assumed. Structural constraints are assumed to limit the maximum acceptable wing root bending moment to 800kNm as well as the maximum wing loading (W/S) to 430kg/m^2. Additionally, the static

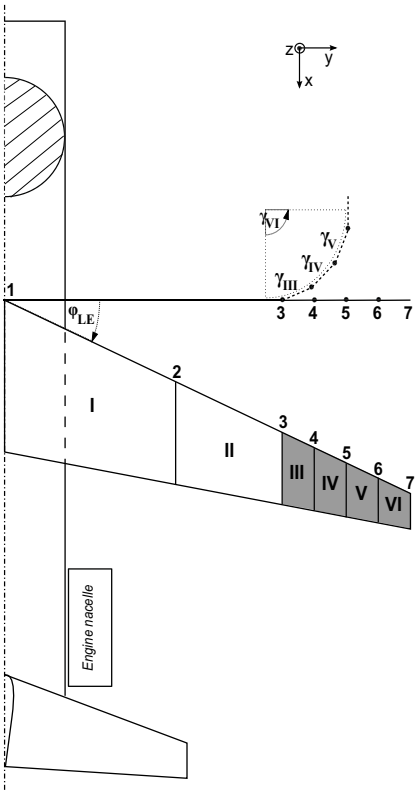

FIG 1: Parametrization of the simulation reference model.

longitudinal aircraft stability margin $(x_n – x_{c.g.})/c_{ref}$ has to exceed at least 5%. Configuration angle of attack (AoA) are constrained to the range of -2 to 8° to meet the requirements for the application of linear aerodynamics.

3.2 Aircraft Model

The aircraft model includes the following major aircraft conceptual design disciplines (see also FIG. 3):

- Geometry
- Aerodynamics
- Structures
- Weight and Balance
- Trim and Stability
- Propulsion

All disciplines are implemented within enclosed design modules that interact with each other to calculate basic rigid aircraft performance characteristics like thrust to weight ratio (T/W), wing loading (W/S) or lift to drag ratio (L/D) as a function of geometry and flight conditions. The modeling focus is on the aircraft wing due to the morphing wing-tip which has been considered by a higher level of detail. As an application of the aircraft model, a parametric aircraft design analysis can be performed to define an aircraft operating range within feasible combinations of (T/W) and (W/S) which simultaneously fit the operational requirements like take-off field length or minimum speed.

In FIG. 1, the considered aircraft component geometries for drag calculation as well as the wing geometry parametrization is shown. Fuselage and engine nacelles are modeled as simple cylindrical bodies of revolution parameterized by length and diameter (see FIG. 1). Lifting surfaces (wing, vertical and horizontal tail) are modeled with a single trapezoid planform. The wing geometry is composed of 6 trapezoid wing partitions with 7 corresponding wing sections. Each wing section is specified by a 4-digit NACA airfoil notation, defining camber δ and relative thickness (t/c) as well as airfoil maximum lift. Equation (1) [21] describes the local wing section maximum lift as a function of camber δ, relative airfoil thickness (t/c) and the position of maximum camber p (40% at 4-digit NACA airfoils) and is also used to calculate the lift dependent profile drag contribution (see Chapter 4).

TAB 2: Morphing wing-tip degrees of freedom (DoF).

Wing-tip DoF	Lower bound	Upper bound
Twist (ε)	-6°	+6°
Camber (δ_{out})	0%	9%
Cant angle (γ)	-85°	+85°

$$c_{l,max} = 1.67 + 7.8\ p\delta - 2.6\ \frac{(0.123 + 0.022\ p - 0.5\ \delta - (t/c))^2}{(t/c)^{2/3}} \quad (1)$$

The wing partitions I and II with a span of 6.8m are referred as the base wing. The wing partitions III-VI added to the base wing represent the morphing wing-tip with a span of 3.2m and the DoF given in TAB. 2.

These morphing wing-tip DoF can be continuously modified within the defined upper and lower bounds also given in TAB. 2. This avoids penalties due to discontinuities and leads to smooth wing-tip shape changes with beneficial aerodynamic properties. Furthermore, these quasi continuous shape changes are more accurate to emulate different morphing technologies.

To reduce the number of the independent wing-tip DoF to the basic parameter

- twist,
- camber,
- and cant angle,

a suitable wing-tip geometry parametrization combined with corresponding geometry change rules is introduced. The control of the wing-tip deflections is achieved by changing the geometry and position of the outer wing section 7 only (wing-tip shape control section).

Tip twist ε is modeled as linear span-wise change of the local airfoil section incidence angle, described by Eq. (2). Therein, $\varepsilon(b)$ represents the twist as a function of wing span b, aerodynamically modeled by changing the local airfoil section incidence flow. Section 7 controls the twist ε_7 for the remaining wing-tip sections.

$$\varepsilon(b) = \frac{(b - b_3)}{(b_7 - b_3)}\ \varepsilon_7 \quad (2)$$

The camber δ_{out} of the NACA 4-digit airfoil sections can be continuously modified ranging from 0 to 9% synchronously for all wing-tip sections (3-7). If camber is applied, the airfoils always feature a constant maximum camber position at 40% of the airfoil chord length. Thus, an applied camber of 4% with an assumed relative wing thickness (= relative airfoil thickness) of 12% results in a discrete NACA 4412 airfoil.

Non-planar wing-tip geometries can be modeled by deflecting the wing-tip partitions III-VI out off plane (up- or downwards)

according to a circular arc approximation (see FIG. 1). The cant angle of the outer partition VI $\gamma_{(VI)}$ is measured from the x-y-plane to the wing-tip partition VI. All other section cant angles are obtained according to the following scheme:

$$\gamma_{(\mathrm{III})} = 0.25\ \gamma_{(\mathrm{VI})} \quad (3)$$

$$\gamma_{(\mathrm{IV})} = 0.5\ \gamma_{(\mathrm{VI})} \quad (4)$$

$$\gamma_{(\mathrm{V})} = 0.75\ \gamma_{(\mathrm{VI})} \quad (5)$$

Primary aerodynamic benefits of morphing wing-tips are apparent in terms of induced drag reduction and load control. This depends on the span-wise distribution of lift as a function of the wing geometry. A vortex-lattice method is used to calculate the lift distribution of the complex non-planar wing geometries and the induced drag distribution along the span to determine essential aerodynamic coefficients and derivatives like wing pitching moment c_m or roll damping c_{lp}. The Athena Vortex Lattice software tool AVL developed by *Drela* and *Youngren* [22] applies a single-layer vortex sheet, discretized into horse-shoe vortex filaments which are used to determine all relevant aerodynamic coefficients and derivatives. To ensure a high wing model resolution and to capture a smooth surface pressure distribution particularly at the wing-tips, 100 span-wise and 9 chord-wise wing panels are set. Since the lift distribution of the wing is known, the forces acting on each span-wise wing panel are also used to calculate the structural loads as a function of the wing geometry and flight state within the structure module. As an output of the structure module, the total wing root bending moment, wing loading and mass moment of inertia are calculated.

Zero-lift drag contributions to the aircraft total drag are considered for each aircraft component separately (see FIG. 1) by profile and friction drag as well as by wave drag due to shocks and boundary layer effects.

The applied aerodynamic modeling methods limit the validity of the aircraft model to linear aerodynamics which is satisfied at small angles of attack (AoA). Additionally, no boundary layer or flow separation effects are considered. Compressibility effects are treated by using the Prandtl-Glauert transformation which limits the maximum free-stream Mach number to transonic regimes.

Figure 2 shows typical wing configurations generated by the geometry module and transmit to the aerodynamic module.

FIG 2: Different settings of the morphing wing-tip DoF.

The weight and balance module calculates the aircraft overall center of gravity (c.g.) as a function of wing geometry, fuel load and payload. Additionally, the aircraft configuration is trimmed around its c.g. within an iterative trim routine by adjusting the horizontal tail incidence. With the known trimmed AoA, the longitudinal static stability of the actual aircraft configuration can be determined. The resulting total aircraft configuration trimmed drag force and the corresponding flight conditions represent the thrust demands for the propulsion system during non-accelerated flight states. The propulsion system model is provided by the BADA engine performance model [23] and consists of two Rolls-Royce AE3007A1 turbo-fan engines.

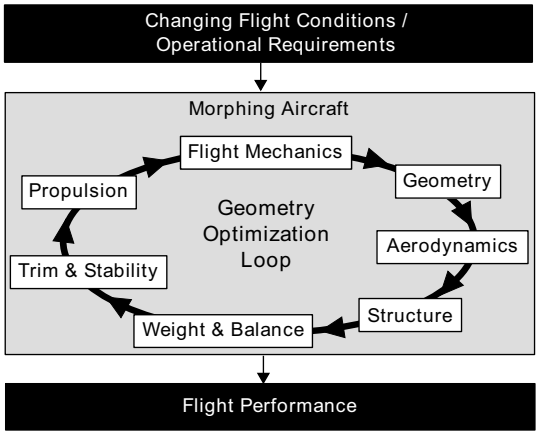

FIG 3: Morphing simulation model featuring a geometry optimization loop to improve specific aircraft performance characteristics.

3.3 Simulation Model

An aircraft mission performance simulation requires information about aerodynamic, structural and propulsion system performance characteristics as a function of changing flight conditions. For rigid aircraft with fixed performance characteristics, such a data set can be easily generated from the output of the aircraft conceptual design process.

When considering morphing within a simulation model, the aircraft performance characteristics can be optimized for changing flight conditions and specific flight segment objectives. To achieve this, the introduced aircraft model is extended by a flight mechanics module and a gradient-based optimization algorithm shown in FIG. 3. This automatized closed loop optimization routine, including all relevant aircraft design modules, enables the calculation of the optimum morphing wing-tip geometry and the corresponding overall aircraft performance depending on specific flight conditions.

In FIG. 3 an overview of the entire simulation model including the aircraft design modules and their interaction towards a closed loop optimization is given. All modules as well as the optimization routine are implemented in Matlab and can be controlled and monitored via user interface.

The input of the model is described by discrete flight state parameters extracted from the mission trajectory like altitude, speed or bank angle as well as specific flight segment objectives like maximization of rate of climb or maximization of cruise speed. Operational mission requirements determine the mission fuel and payload as well as the flight operation envelope (speed vs. altitude).

This information is processed within the flight mechanics

module into concrete flight performance optimization objectives like minimization of total drag or maximization of lift. Additionally, constraints like maximum root bending moment or required lift coefficients to overcome the aircraft weight are considered to ensure feasible flight states. A gradient-based optimization routine (Matlab Fmincon) is applied to the wing-tip geometry to satisfy a specific optimization objective while simultaneously fulfilling the constraints. Potential wing-tip DoF parameter combinations, generated by the optimizer, are passed to the geometry module to generate an entire wing geometry which is then successively passed to all other modules (see FIG. 3).

The optimization routine will be terminated as soon as the optimum wing-tip geometry is found by fulfilling the convergence criteria while the constraints are satisfied. Within the flight mechanics module, the output of the simulation model is finally determined in terms of the optimum flight performance including all relevant aircraft characteristics. Additionally, the aircraft trajectory (path- and bank angle) and fuel burn is calculated for a previously defined constant time step.

A key enabler for a fast and continuous simulation model response are surrogate models which are applicable to generate continuous approximation models from n-dimensional discrete training data. Noticeable advantages of surrogate models can be summarized as follows:

- Fast system response and computational efficiency.
- Easy handling and integration into existing models.
- Processing and conversion of discrete input data into continuous output.

Thus, surrogate modeling is an advantageous method in regard to model design space explorations or mission performance simulations, where precise system results from higher order simulations need to be accessible without recourse to use the primary source. On the other hand, aircraft mission simulations frequently require continuous outputs (e.g. lift or drag) as a function from n-dimensional input data (e.g. aircraft geometry and flight state).

The scientific challenge of surrogate modeling is to achieve a best possible accuracy at limited number of simulation evaluations. This depends highly on the selection of appropriate sampling data as well as the selection of an adequate surrogate modeling method including its parameter settings. For the present 12-dimensional problem, a design of experiments (DoE) including 10,000 points has been selected as the input for the surrogate model. An optimized 12-dimensional Latin Hypercube (LHC), including all DoE data points has been used to generate a sampling plan. Besides the three morphing wing-tip DoF (see TAB. 2), the remaining model dimensions are the aircraft flight state parameters, basic wing aircraft geometry data like inner wing camber, chord length or wing thickness. This is required for example to emulate a high-lift system for mission simulation by changing inner wing camber and wing chord length accordingly or to search for an optimum reference configuration for a desired design mission. Feed-forward Artificial Neural Networks (ANN) with up to 85 neurons per hidden layer have been used to generate various surrogate models to map the aircraft characteristic as a function of 12 parameter dimensions. The approximation performance of the generated surrogate model is measured by the root mean square error (RMSE) of each configuration parameter r:

$$\mathrm{RMSE}\ (\mathrm{r}) = \sqrt{\frac{\sum_{\mathrm{i}=1}^{\mathrm{n}} (\mathrm{r} - \widehat{\mathrm{r}})^2}{\mathrm{n}}} \qquad (6)$$

TAB 3: Surrogate model validation.

Config. Parameter	Number of Neurons	RMSE	Typical Values	Related Error
c_L [-]	70	2.09E–03	0.5	0.42 %
$c_{Di,w}$ [-]	70	1.99E–04	0.02	1.00 %
$M_{b,root}$ [Nm]	40	1.24E+04	1.0E+06	1.24 %

For RMSE calculation and thus for surrogate model validation, $n = 100$ additional arbitrary simulation data sets, which have not been used for training the ANN are generated via an additional LHC. The presented RMSE in TAB. 3 show acceptable model performances for the present problem. Note, that the validation is conducted including all 12 dimensions. For the 6-dimensional morphing wing-tip problem (v_{tas}, Alt, α, ε, δ_{out}, γ), the model boundaries exceed the relevant design space, which further improves the approximation. Moreover, a parameter design space study of the surrogate model response, which covers the whole design space shows smooth behavior which is required for gradient based optimization algorithm. In FIG. 4 relevant aircraft characteristics are plotted versus a continuous variation of the morphing wing-tip parameters ε, δ_{out} and γ from the lower to the upper defined model bound. Results presented in FIG. 4 refer to a symmetrically deflection of both, the left- and the right wing-tip and are not trimmed around the aircraft c.g. During single parameter morphing, the remaining wing-tip geometry parameters are fixed and represent the rigid reference configuration, introduced in chapter 4 (see TAB. 4). Additionally, the effect of changing solely the aircraft AoA from -1 to 5° is plotted in FIG. 4 as a dashed line. It can be pointed out that in general the morphing wing-tip effectiveness to manipulate the aircraft characteristics is relatively small compared to the AoA influence. A major reason for that is the relatively small total wing-tip surface area of 18% of the total wing area. Additionally, the span-wise lift distribution of the wing steeply drops to zero at the wing-tips which further significantly decreases the influence of the wing-tips to alter the global lift distribution. This is in particular expressed in the c_L plot where changes in AoA significantly affecting the total wing lift coefficient. Thus, modifications of the camber of the inner wing sections are much more effective in changing aircraft characteristics but result at the same time in an increased aircraft drag, also seen in the c_{Di} and c_{Dp} plots. The morphing parameter "cant angle" shows significant effectiveness to decrease the aerodynamic roll damping c_{lp}, which is important when aircraft agility is considered.

4 Results

Adaptive or morphing wing-tip devices are capable to maintain optimum geometry for minimum induced drag at given lift over a broad range of operational conditions.

The focus of the conducted flight performance studies at fixed flight conditions (Alt=20kft, Ma=0.5, $\mathrm{M_{A/C,tot}} = 20$t) is to analyze the potential of a morphing wing-tip to reduce induced drag but also morphing functionalities given in TAB. 5.

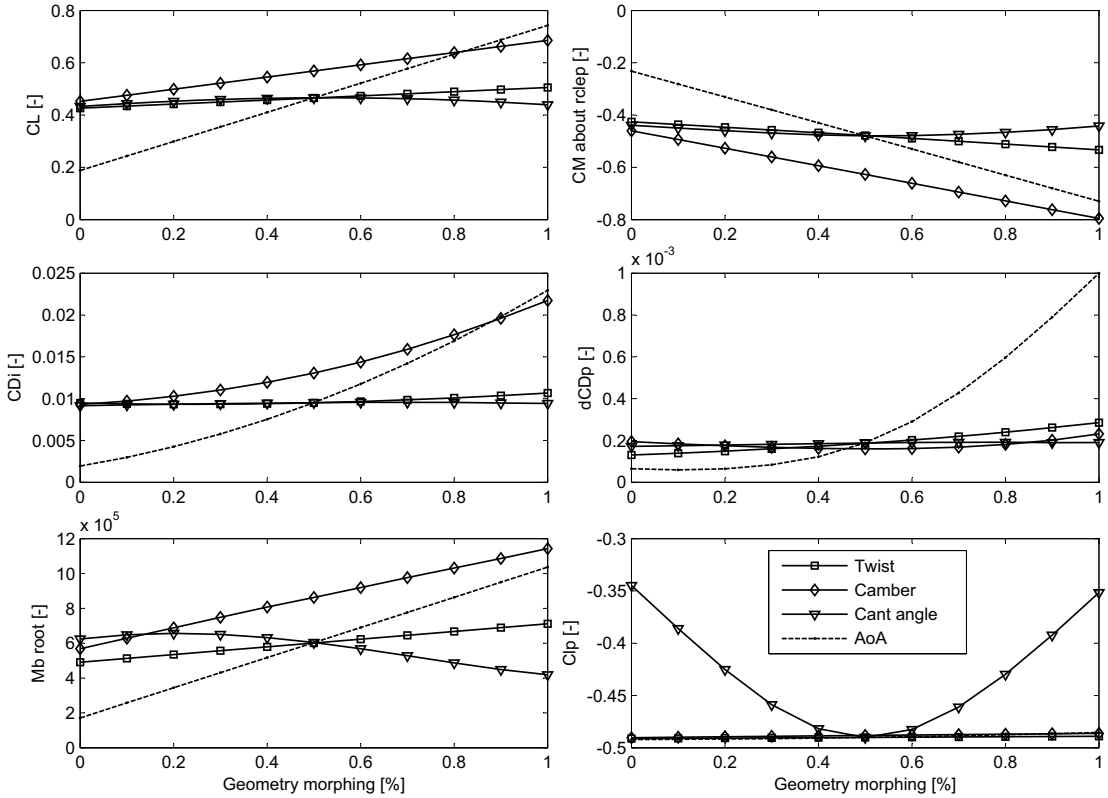

FIG 4: Surrogate model response of selected aircraft characteristic parameter. The geometry morphing of the single morphing parameter ranges from the lower- to the upper surrogate model bounds.

4.1 Flight Performance

For the assessment of morphing benefits, an optimum rigid reference configuration is required. A design mission (see FIG. 8) has been defined to optimize the wing geometry parameters, base wing camber δ_{in} (sections 1-2), wing-tip camber δ_{out}, twist ε, and cant angle γ (sections 3-7) in order to minimize the overall mission fuel burn and thus to find the reference configuration parameter. This four-dimensional optimization problem is implemented via using a genetic algorithm (Matlab Genetic Algorithm Toolbox) featuring 30 populations applied to 20 generations. The advantage of using a stochastic optimization algorithm is that morphing wing-tip geometry combinations which are not representing feasible solutions (e.g. when aerodynamic drag at high speed cruise overcomes available engine thrust) are neglected and do not impair the optimization result. Only feasible wing parameter combinations having best performance and thus lowest mission fuel burn, survive and become the parents for the next generation. The results of the wing parameter optimizations for the design mission (see FIG. 8) is shown in TAB. 4.

TAB 4: Design mission wing geometry optimization with minimum fuel burn as the objective to define a rigid reference configuration.

Wing geometry DoF	Lower bound	Upper bound	Mission opt. value
Base wing camber (δ_{in})	0%	9%	3.47%
Wing-tip camber (δ_{out})	0%	9%	0.53%
Twist(ε)	-6°	+6°	0.14°
Cant angle (γ)	-85°	+85°	0.09°

The most suitable way to demonstrate the effect of induced drag reduction for specific flight speed and altitude combination is to calculate the trimmed induced drag polar. The upper left panel of FIG. 5 shows the induced drag reduction c_{Di} due to the wing-tip morphing as a result of an optimization problem. The trimmed rigid drag polar in FIG. 5 is generated by varying the configurations AoA systematically from 0 to 7° including the application of a trim routine to compensate the configuration's pitching moment around c.g. by deflecting the horizontal tail. The resulting total configuration lift coefficients c_L simultaneously represent the required lift coefficients $c_{L,req}$ for each morphing wing-tip optimization case. A gradient based optimizer (Matlab Fmincon) is applied to optimize the wing-tip geometry parameter δ_{out}, ε, and γ in order to reduced induce drag at given lift coefficients and for trimmed conditions ($c_m^{c.g.} = 0$). The numbers in the top left chart of FIG. 5 show the obtained induced drag reduction as a function of the morphing parameters which are plotted versus $c_{L,tot}$ on the bottom row of FIG. 5. In general, the parameters δ_{out}, ε, and γ are continuously adjust in order to generate the required total lift at lower trimmed AoA, see top right chart of FIG. 5. An instantaneous effect of lowering the trimmed AoA is a decrease in lift-dependent profile drag contribution Δc_{Dp} (see the top row mid panel of FIG. 5). This can be explained as the offset of the actual configuration lift coefficient $c_{L,tot}$ relative to the design lift coefficient of the entire wing $c_{L,D}$. The total wing

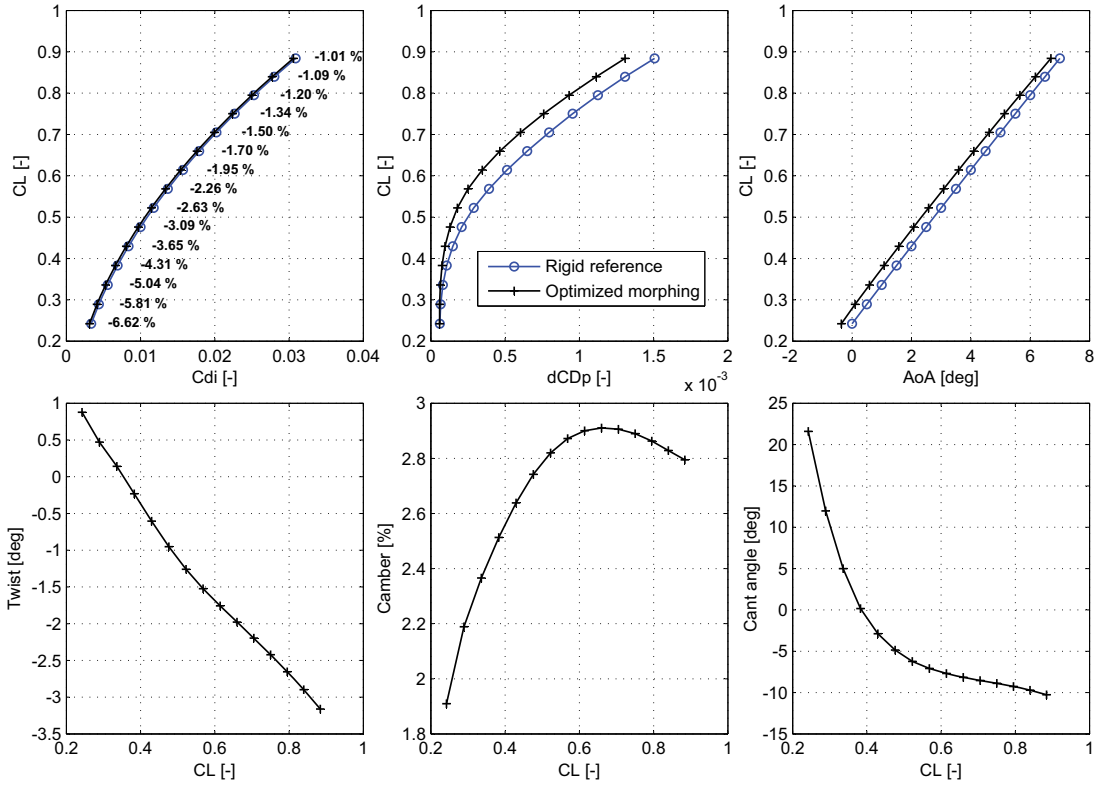

FIG 5: Induced drag study of a rigid reference configuration compared to a morphing wing-tip including variable twist, camber and cant angle.

lift dependent profile drag contribution can be calculated by the span-wise local lift coefficients c_l taken from AVL and the local section $c_{l_{max}}$ with Eq. (1) and (7) [17].

$$\Delta c_{Dp} = 0.75(0.01 c_{l_{\max}} - 0.0046(1+2.75\,(t/c)) \left(\frac{c_l - c_{l_i}}{c_{l_{\max}} - c_{l_i}} \right)^2 \tag{7}$$

for Re $> 10^7$

However, the increase of wing camber results significantly in an increase of the wing pitching moment c_m (see FIG. 4) and thus to an increase of the required negative lift at the horizontal tail for trimming. This instantaneous effect influences the total configuration's trimmed drag polar and inhibit the exploitation of the maximum overall drag reduction potential of wing-tip devices. Thus, to exploit the maximum drag reduction potential, the total configuration drag accounting for all drag contributing aircraft components at trimmed condition should be selected as the optimization objective.

Besides the in-flight drag reduction (mission adaptive wing MAW) potential of morphing wing-tips, additional flight performance improvement referred to the areas of wing aerodynamics and structural loads have to be taken into account:

- Increase of aircraft maneuverability by exploit the capability of a morphing-wing tip to generate additional lift.
- Improvement of the aircraft agility by a reduction in aerodynamic roll-damping or moment of inertia.
- Aerodynamic load reduction especially during maneuvering (maneuver load control MLC).

From these potential benefits, performance metrics can be easily derived to quantify specific morphing benefits over a broad range of application.

TAB 5: Performance metrics for morphing benefit assessment.

Morphing Functionality	Derived Metric	Optimization Objective
MAW	Total config. drag	$c_{D,tot}$
Maneuverability	Max. bank angle	$c_{L,max}$
Agility	Roll damping	c_{lp}
MLC	Root bend. moment	$M_{b,root}$

Figure 6 shows the results of the optimization scenarios shown in TAB. 5. Thus, the settings of the morphing wing-tip DoF are adjusted in order to achieve maximum aircraft performance improvements, while neglecting other performance characteristics. The results are presented as trimmed total configuration drag polars, maximum lift $c_{L,max}$ vs. systematically adjusted configuration AoA ranging from -2 to 7°, and configuration roll-damping coefficients c_{lp} as well as the resulting dimensionless root bending moments $m_b = \left(\frac{M_b}{\rho/2\ v^2\ S_{ref}\ b_{ref}} \right)$ versus $c_{L,req}$. Additionally, the optimum rigid reference configuration performance characteristic is plotted for assessment purposes. Figure 7 shows the corresponding optimized wing-tip parameter settings versus $c_{L,req}$. The top left chart shows the dimensionless performance improvements in percent, relative to the rigid reference configuration. As expected, large performance improvements due to morphing are achievable in distinctive off-design regimes of the rigid reference configuration.

However, the results given in FIG. 7 are specific aircraft

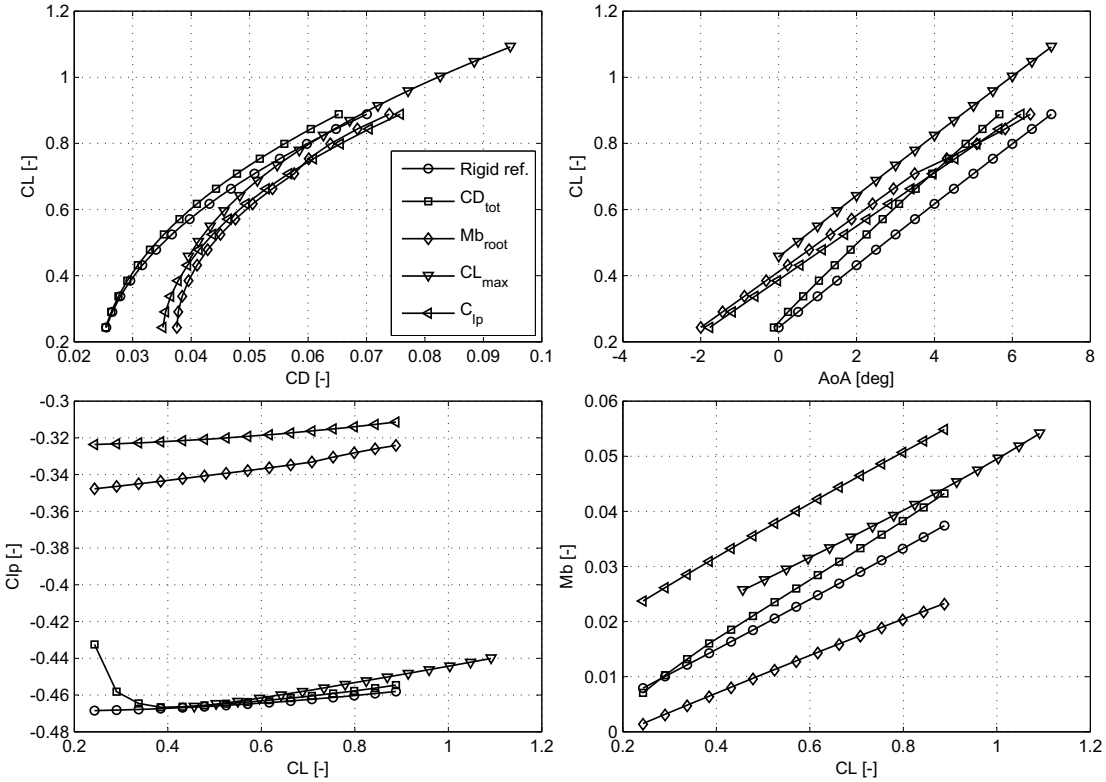

FIG 6: Morphing flight performance results for various aerodynamic- and structural optimization objectives.

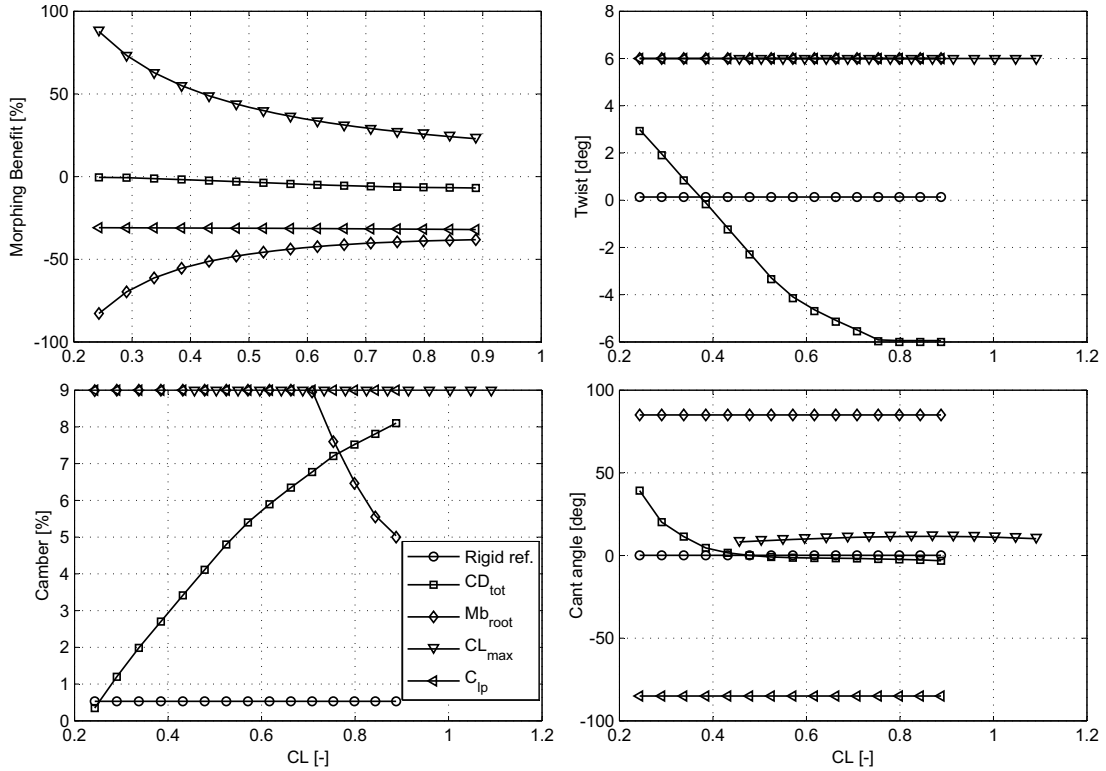

FIG 7: Performance benefits of morphing as a function of the morphing geometry parameters.

flight performances at a specific flight state, aircraft mass and c.g. position. For a comprehensive morphing net-benefit assessment the overall mission performance benefits at changing flight conditions and for various mission segment optimization objectives have to be considered.

4.2 Mission Performance

The above discussed flight performance benefits of a morphing wing-tip are now applied to an aircraft mission including divergent mission segments (see FIG. 8). These mission segments include also different flight performance objectives given in TAB. 5 to demonstrate the operational performance benefits for wide range of applications.

Starting at sea level, the climb profile to 37kft is composed of three climb segments with a changing speed schedule. Here, the flight segment optimization objectives are to maximize rate of climb and thus to reduce total configuration drag. During high speed cruise at 37kft with Ma=0.78, as well as for loitering at 26kft the optimization objective is to minimize fuel burn. At 6.6kft, a 360° right turn shows the ability of the morphing wing tip to maximize lift, demonstrated via the maximization of the aircraft bank angle and thus the turn rate. The following 100nm level flight section is intended to adapt the wing-tip geometry in order to provide a low aerodynamic damping coefficient c_{lp} to allocate the aircraft an improved agility. Within the next mission segment the aircraft performs a 360° left turn at constant aircraft bank angle of 45°, showing the morphing wing-tip ability to minimize the wing root bending moment.

For mission performance analysis, the defined multi-objective mission simulation is accomplished by the rigid reference configuration, each single morphing DoF and for the all-morphing case where all morphing DoF are optimized simultaneously.

A dimensionless morphing efficiency η_{morph}, developed in [15] is applied to each mission segment to calculate a dimensionless morphing parameter efficiency of each morphing wing-tip DoF.

The absolute measure of any morphing wing-tip concept benefit with respect to the rigid reference case is

$$\Delta F_{\text{benefit}} = F_{\text{morph}} - F_{\text{rigid}} \tag{8}$$

the absolute measure of the maximum achievable benefit of a fully morphing wing-tip in respect to the rigid reference is

$$\Delta F_{\text{max.benefit}} = F_{\text{all-morph}} - F_{\text{rigid}} \tag{9}$$

The morphing impact efficiency is defined as the percentage of the morphing benefit that is achieved with respect to the rigid reference and the all-morphing optimum case:

$$\eta_{\text{morph}} = \frac{F_{\text{morph}} - F_{\text{rigid}}}{F_{\text{all-morph}} - F_{\text{rigid}}} = \frac{\Delta F_{\text{benefit}}}{\Delta F_{\text{max.benefit}}} \tag{10}$$

If multiple mission segments are considered, the total morphing efficiency can be calculated with

$$\eta_{\text{morph,tot}} = \sum_{i=1}^{n} k_i \ \eta_{\text{morph,i}} \quad \text{with} \sum_{i=1}^{n} k_i = 1 \tag{11}$$

whereas k_i represents a weighting factor to account for mission segment optimization priorities. The simulation results for the different optimizations objectives "fuel burn", "maneuverability", "agility", and "wing load" of the morphing cases "twist", "camber", "cant angle", and "all-morph" as well as for the rigid

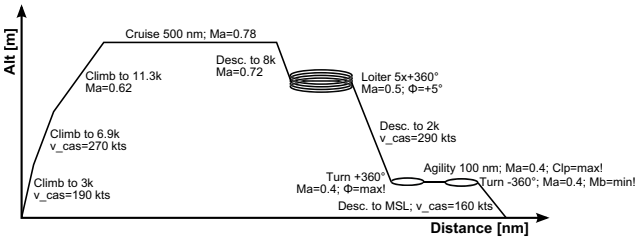

FIG 8: Design mission trajectory including divergent mission segment optimization objectives.

TAB 6: Mission morphing efficiency of single morphing DoF (non-weighted k_i=const.).

Morphing DoF	Cumulated total benefit [%]	Total morphing efficiency [%]
Twist (ε)	10.9	86.2
Camber (δ_{out})	4.9	109.6
Cant angle (γ)	38.4	99.3
All-morph (ε,δ_{out},γ)	75.8	400

reference configuration are presented in FIG. 9. Therein, the grey bars represent the absolute performance benefits compared to the rigid reference configuration. Most absolute benefits can be achieved for wing load reduction which is primarily a function of wing planform. For maneuverability improvements where the maximization of the c_l, max was the optimization objective, wing-tip morphing in general has no significant effect. One reason is the small contribution of the wing tip to the overall lift of the entire wing. However, when considering an entire mission including different mission segment objectives, the absolute contributions of each particular morphing DoF have only limited significance for the single morphing technology assessment in context of morphing. Therefor, the dimensionless single morphing parameter impact efficiency, according to Eq. (10) is also given in FIG. 9. Note, the morphing efficiency for the all-morphing case always represents the theoretical maximum potential of 100%.

In FIG. 10 the mission optimization scenarios accomplished for the optimization parameter ε, δ_{out} and γ are plotted versus mission duration. Additionally, the "all-parameter" optimization case and the rigid reference is plotted within each single morphing optimization case.

With the results in FIG. 9, the non-weighted overall morphing efficiency for each morphing DoF can be calculated with equation (11).

In TAB. 6 the cumulated total performance benefits of each single morphing parameter with respect to the optimum rigid reference performance is present. If all mission segments are equally weighted ($k_i = 1/4 \rightarrow \sum_{i=1}^{4} k_i = 1$), the single morphing wing-tip DoF "cant angle" (γ) yields the highest overall benefit. Although all morphing parameter achieve comparable efficiencies but the parameter "camber" yields most of the available morphing potential which is achieved when all morphing parameter are optimized simultaneously.

Considering the cumulated total benefit of the all-morphing case compared to each single morphing parameter optimization in TAB. 6, a delta performance of 301% is achieved. A

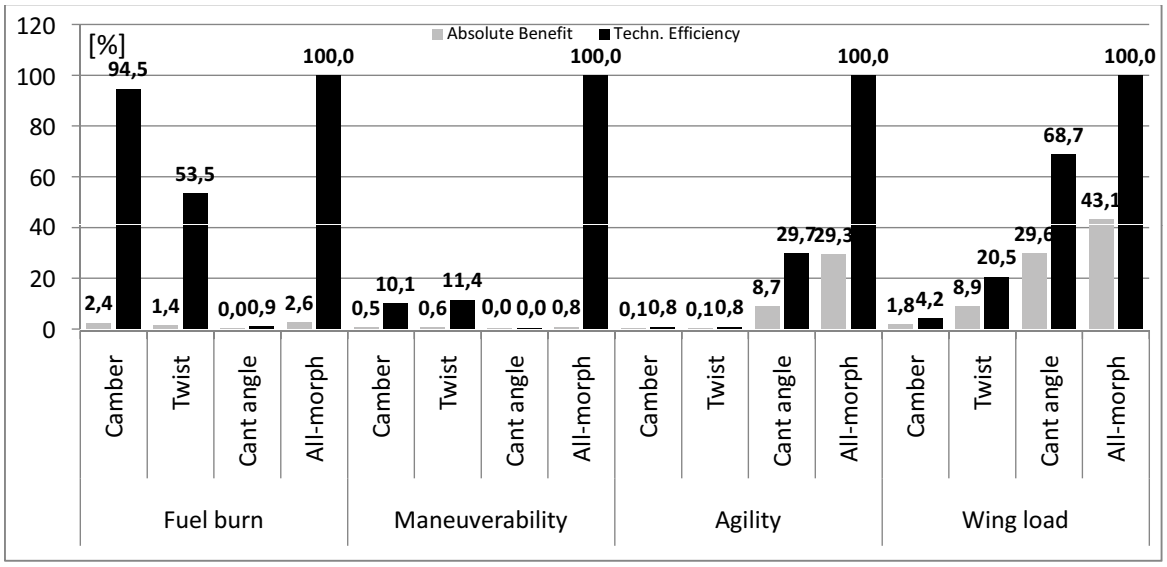

FIG 9: Flight performance improvements due to morphing, calculated for multi-objective mission segment optimizations.

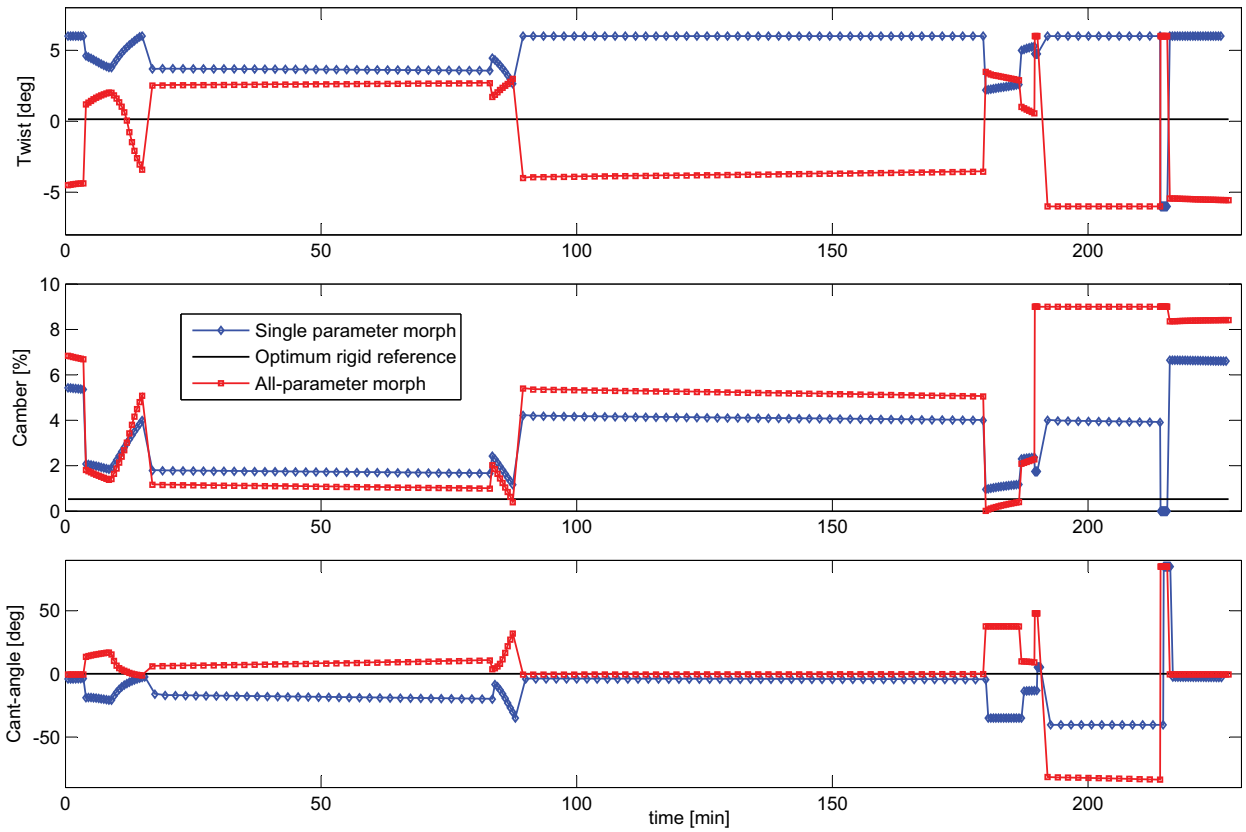

FIG 10: Morphing parameter settings vs. mission duration for different optimization scenarios of a multi-objective mission simulation.

reason therefor are the synergy effects between the single morphing parameters which is most significant for the "wing load" optimization scenario.

5 Conclusion

This paper presents the potential of a morphing wing-tip to improve the flight performance of an aircraft for a broad range of applications compared to a optimum rigid reference wing. A modeling approach for a morphing wing-tip featuring such geometric degree of freedom as twist, camber and cant-angle has been developed and integrated into an overall aircraft simulation model. The simulation model includes a closed-loop gradient based optimization algorithm which enables the morphing wing-tip to adapt its geometry according to arbitrary performance improvement objectives. A flight performance analysis shows the aerodynamic morphing benefits for the optimization scenarios "mission adaptive wing", "maneuverability", "maneuver load control", and for improving the aircraft agility by optimizing the aircraft characteristic "aerodynamic roll damping". A mission simulation including multi-objective mission segments have been conducted to demonstrate a methodology for the overall mission benefit assessment of morphing in general. Additionally, each single morphing parameter contribution in relation to the optimum all-morphing reference is present via dimensionless single parameter morphing efficiencies. The cumulated absolute benefit of the all-parameter morphing reference including all mission segments is 75.8% and represents the absolute morphing benefit with respect to the optimum rigid reference. The most impacting single morphing parameter exploiting most of the morphing potential is the wing-tip camber which achieves 110% of the maximum morphing potential of 400% when four different mission segment optimizations are considered.

A net-benefit assessment for morphing wing-tips can be achieved by applying this framework for weight sensitivity analysis on aircraft level to account for morphing technology weight penalties. Additionally, the introduction of a morphing control in order to minimize the morphing frequency and amplitudes during a mission can be considered to lower the actuator requirements and thus the actuator mass. This can provide a technology push and pull for the most promising morphing developments.

Acknowledgement

This work has been partly supported by Airbus Germany, EADS Defence and Security Military Air Systems and EADS Innovation Works.

Disclamer

Aircraft performance data contained herein are based on data drawn from the EUROCONTROL Base of Aircraft Data (BADA). It is to be noted that the aircraft performance models and data contained in BADA have been developed by EUROCONTROL from a set of aircraft operational conditions available to EUROCONTROL. EUROCONTROL has validated BADA aircraft models only for those conditions and can therefore not guarantee the model's accuracy for operating conditions other then the reference conditions.

References

[1] C. D. Cone. The theory of induced lift and minimum induced drag of nonplanar lifting systems. *NASA-TR-R-139*, 1962.

[2] R. T. Jones. Effect of winglets on the induced drag of ideal wing shapes. *NASA-TM-81230*, 1980.

[3] R. T. Whitcomb. A design approach and selected wind-tunnel results at high subsonic speeds for wing-tip mounted winglets. *NASA-TN-D-8260*, 1976.

[4] P. Marks. Morphing winglets make for greener aircraft. *Newscientist*, 2692, 2009.

[5] V. Wehrtmann and M. Kordt. Konzept eines variablen winglets zur lateralen lastenreduktion zur kombinierten lateralen und vertikalen lastenreduktion und zur performanceverbesserung von fortbewegungsmitteln. Number DE 102005028688 A1 2006.11.30. Airbus Deutschland GmbH, 2006.

[6] M. Sankrithi and J. Frommer. Controllable winglet. Number US 2008/0308683 A1. The Boeing Company, 2008.

[7] J. Perez-Sanches. Verstellmechanismus fuer einen formadaptiven fluegel. Number DE 10317258 B4 2006.09.07. EADS Deutschland GmbH, 2003.

[8] J. B. Allen. Articulating winglets. Number US0005988563A. McDonnell Douglas Corporation, 1999.

[9] N. M. Ursache. Morphing winglets for aircraft mulit-phase improvement. *7th AIAA Aviation Technology, Integration and Operations Conference (ATIO), Belfast, Northern Ireland*, 2007.

[10] P. Bourdin, A. Gatto, and M. I. Friswell. Performing co-ordinated turns with articulated wing-tips as multi-axis control effectors. *The Aeronautical Journal*, 114:13, 2010.

[11] P. Bourdin, A. Gatto, and M. I. Friswell. Aircraft control via variable cant-angle winglets. *Journal of Aircraft*, 45:10, 2008.

[12] J. B. Davidson, P. Chawalowski, and B. S. Lazos. Flight dynamic simulation assessment of a morphable hyper-elliptic cambered span winged configuration. *AIAA Atmospheric Flight Mechanics Conference and Exhibit, Austin, TX*, 2003.

[13] B. S. Lazos and K. D. Visser. Aerodynamic comparision of hyper-elliptic cambered span (hecs) wing with conventional configurations. *20th AIAA Applied Aerodynamics Conference, San Francisco, CA*, 2006.

[14] H.P. Monner, M. Sinapius, and S. Opitz. Dlr morphing activities within the european network. *NATO Research and Technology Organisation (RTO) - Applied Vehicle Technolgy Panel Symposium*, RTO-MP-AVT-168 AC/323(AVT-168)TP/268, 2009.

[15] J. Wittmann, H.-J. Steiner, and A. Sizmann. Framework for quantitative morphing assessment on aircraft system level. *50th AIAA/ASME/ASCE/AHS/ASC Structures, Structural Dynamics, and Materials Conference, Palm Springs, California*, 2009.

[16] D.E Hoak. Usaf stability and control datcom. Technical report, McDonnell Douglas Corporation, Douglas Aircraft Devision, 1969.

[17] Egbert Torenbeek. *Synthesis of Subsonic Airplane Design*. Delft University Press, Kluwer Academic Publishers, 1982.

[18] D. P. Raymer. *Aircraft Design: A Conceptual Approach*. American Institute of Aeronautics and Astronautics, Inc., 4 edition, 2006.

[19] Embraer. *EMB145: Airport Planning Manual*, 2007.

[20] J. Jenkinson, P. Simpkin, and D. Rhodes. *Civil Jet Aircraft Design*. Butterworth Heinemann, 1999.

[21] B. W. McCormick. *Aerodynamics Aeronautics and Flight Mechanics*. John Wiley & Sons, Inc., 1995.

[22] M. Drela and H. Youngren. *AVL 3.26 User Primer*. MIT Aero and Astro and Aerocraft Inc.

[23] Eurocontrol. *User Manual For the Base of Aircraft Data (BADA) Revision 3.7*. European Organisation for the Savety of Air Navigation - Eurocontrol Experimental Centre, 3.7 edition, 2009.